

A Relativistic Parton Cascade with Radiation

Ghi R. Shin^{†‡} and Berndt Müller[‡]

[†] Department of Physics, Andong National University, Andong, South Korea

[‡] Department of Physics, Duke University, Durham, NC 27708-0305, USA

Abstract. We consider the evolution of a parton system which is formed at the central rapidity region just after an ultrarelativistic heavy ion collision. The evolution of the system, which is composed of gluons, quarks and antiquarks, is described by a relativistic Boltzmann equations with collision terms including radiation and retardation effects. The equations are solved by the test particle method using Monte-Carlo sampling. Our simulations do not show any evidence of kinetic equilibration, unless the cross sections are artificially increased to unrealistically large values.

PACS numbers: 25.75.+r

1. Introduction

The possible formation and evolution of a quark-gluon plasma (QGP) in relativistic heavy-ion collisions has been an important and very active research subject in recent years. Besides the theoretical studies of possible signatures of QGP formation, many investigations have been concerned with space-time dynamics of the QGP, its formation and final decay into hadrons. Perhaps the most common description of the evolution of the QGP has been based on relativistic hydrodynamics [1, 2]. This approach, however, does not address many important issues, in particular, the initial formation and local equilibration of the QGP. To explore this issue theoretically, a microscopic description of the parton system is required, which allows one to follow the phase-space evolution in detail. One such approach is the parton cascade model [3, 4, 5, 6].

An important conceptual problem faced by such microscopic models is that they require a very detailed specification of the initial state. Due to our ignorance of nonperturbative processes in QCD, we do not know how to extract the required information from the parton wavefunctions of the colliding nuclei. Since the original formulation of the parton cascade model, important progress in our understanding of the parton structure of large nuclei at small Bjorken- x physics has been made [7]. There is good reason to believe that the parton distribution at the beginning of a relativistic heavy ion collision can be described by means of semiclassical methods. This improvement of our understanding the initial state has motivated a resurgence of theoretical studies of the microscopic evolution of the matter formed in the central rapidity region in a nuclear collisions [6, 8].

To date, those studies have mostly focused on elastic collisions among partons, although the parton cascade model was originally formulated to include radiative processes as time-like and space-like branchings in the leading logarithmic approximation [3]. It has been pointed recently by Baier et al. [9] that the inelastic $gg \rightarrow ggg$ process is the essential driving force toward the kinetic equilibration of the parton system. The importance of this process for the chemical equilibration of the QGP was already studied and pointed out by Biró et al. [10].

There is also a serious defect in many numerical implementations of the cascade model: the superluminal propagation of interactions [11, 5, 6]. This becomes important whenever the hard-sphere picture of scattering interactions is applied without proper incorporation of the retardated nature of interactions in quantum field theory.

In this article, we develop a cascade code which includes the process($gg \rightarrow ggg$) as well as a relativistic picture of scattering that eliminates the superluminal problem. We assume a boost-invariant initial state and analyze the time evolution of the parton system. Because we do not include a model of the hadronization process, our description is useful only for a few fm/ c after the onset of the reaction.

In section 2 we present the equations of motion describing the evolution of a relativistic system composed of quarks, antiquarks, and gluons. In section 3 we explain the cascade code, especially the choice of the initial state and the parton dynamics. Our

results and conclusions are discussed in section 4.

2. Equations of Motion

We consider here a system, which consists of gluons, quarks (u, d, s) and their antiquarks, formed just after the impact of a heavy ion collision. The typical de Broglie wave length of a particle in the system, $\lambda = \hbar/pc$, is much shorter than the average distance between particles even at relatively high density so that we assume those particles can be considered as relativistic classical particles. We thus assume that the semi-classical but relativistic approach is applicable to this highly energetic and dense parton system. This may not be true for some particle whose energy is less than 1 GeV, but we limit our consideration to observables for which the particle picture is expected to be a good approximation.

The system which we are studying can be described by the Lorentz-covariant Boltzmann equation [12, 13],

$$p^\mu \partial_\mu f(x, \mathbf{p}) = C(\mathbf{x}, \mathbf{p}, t), \quad (1)$$

where $f(x, \mathbf{p})$ is a phase space distribution function and the right-hand side denotes the collision terms. We assume that there is no external force acting on the system and the self-generated forces of the system are fully described by collisions.

Gluons and quarks (u, d, s) and their antiparticles ($\bar{u}, \bar{d}, \bar{s}$) are independent constituents so that the system is a mixture of 7 different kinds of partons. These particles can scatter on each other elastically and they can produce new particles. We will consider here only the dominant processes among many possible ones: $gg \leftrightarrow gg$, $gq \leftrightarrow gq$, $g\bar{q} \leftrightarrow g\bar{q}$, $gg \rightarrow ggg$, $qq \leftrightarrow qq$, $\bar{q}\bar{q} \leftrightarrow \bar{q}\bar{q}$, $q\bar{q} \leftrightarrow q\bar{q}$, $gg \leftrightarrow q\bar{q}$.

Including only those processes among partons, the Boltzmann equation for gluons takes the form:

$$\begin{aligned} p^\mu \partial_\mu f_g(x, \mathbf{p}) = & \int_2 \int_3 \int_4 \frac{1}{2} W_{gg \rightarrow gg} [f_g(3) f_g(4) - f_g(1) f_g(2)] \\ & + \int_2 \int_3 \int_4 W_{gq \rightarrow gq} [f_g(3) f_q(4) - f_g(1) f_q(2)] \\ & + \int_2 \int_3 \int_4 \int_5 \frac{1}{6} W_{gg \rightarrow ggg} [f_g(4) f_g(5) - f_g(1) f_g(2)] \\ & + \int_2 \int_3 \int_4 W_{g\bar{q} \rightarrow g\bar{q}} [f_g(3) f_{\bar{q}}(4) - f_g(1) f_{\bar{q}}(2)] \\ & + \int_2 \int_3 \int_4 \frac{1}{2} [W_{q\bar{q} \rightarrow gg} f_q(3) f_{\bar{q}}(4) - W_{gg \rightarrow q\bar{q}} f_g(1) f_g(2)], \end{aligned} \quad (2)$$

where we used the abbreviated notations $f_g(i) = f_g(\mathbf{x}, \mathbf{p}_i; t)$, $q = (u, d, s)$, $\bar{q} = (\bar{u}, \bar{d}, \bar{s})$, and $f_i = \int d\mathbf{p}_i / E_i$. Note that we assign the label 1 to the momentum \mathbf{p} and set $f_g(1) f_g(2) \rightarrow f_g(3) f_g(4) f_g(5)$ for loss and $f_g(4) f_g(5) \rightarrow f_g(1) f_g(2) f_g(3)$ for gain in $gg \rightarrow ggg$ process. We explicitly include the particle symmetry factor in the classical limit.

We also obtain the evolution equations for quarks and antiquarks,

$$p^\mu \partial_\mu f_q(x, \mathbf{p}) = \int_2 \int_3 \int_4 C W_{qq' \rightarrow qq'} [f_q(3) f_{q'}(4) - f_q(1) f_{q'}(2)]$$

$$\begin{aligned}
& + \int_2 \int_3 \int_4 W_{gq \rightarrow gq} [f_q(3) f_g(4) - f_q(1) f_g(2)] \\
& + \int_2 \int_3 \int_4 \frac{1}{2} [W_{gg \rightarrow q\bar{q}} f_g(3) f_g(4) - W_{q\bar{q} \rightarrow gg} f_q(1) f_{\bar{q}}(2)]. \quad (3)
\end{aligned}$$

$$\begin{aligned}
p^\mu \partial_\mu f_{\bar{q}}(x, \mathbf{p}) & = \int_2 \int_3 \int_4 C W_{\bar{q}\bar{q}' \rightarrow \bar{q}\bar{q}'} [f_{\bar{q}}(3) f_{\bar{q}'}(4) - f_{\bar{q}}(1) f_{\bar{q}'}(2)] \\
& + \int_2 \int_3 \int_4 W_{g\bar{q} \rightarrow g\bar{q}} [f_{\bar{q}}(3) f_g(4) - f_{\bar{q}}(1) f_g(2)] \\
& + \int_2 \int_3 \int_4 \frac{1}{2} [W_{gg \rightarrow q\bar{q}} f_g(3) f_g(4) - W_{q\bar{q} \rightarrow gg} f_{\bar{q}}(1) f_q(2)]. \quad (4)
\end{aligned}$$

where $C = 1/2$ if the final state consist of identical particles and $C = 1$ otherwise. We neglect in these Boltzmann equations those quantum mechanical effects coming from Bose enhancement factors $(1 + f_g)$ for a gluon in the final state and Pauli blocking factors $(1 - f_q)$ for final-state quarks or antiquarks. The quantum transition rates can be expressed in terms of differential cross sections, e.g.

$$W_{gg_1 \rightarrow g'g'_1} = s \sigma^{gg \rightarrow gg}(s, \theta) \delta^{(4)}(p + p_1 - p' - p'_1), \quad (5)$$

where s is the CM energy squared.

These equations are highly non-linear and are impossible to solve analytically even with simplest initial state. To find solutions to these equations, we use the test particle method with Monte-Carlo sampling.

3. Numerical Simulation

The main idea to solve the Boltzmann equations (2, 3, 4) is as follows. We assume that we know the initial state of the system, the position and momentum of each particle at a given time:

$$f(\mathbf{x}, \mathbf{p}, t_0) = \sum_i^N \delta(\mathbf{x} - \mathbf{x}_i(t_0)) \delta(\mathbf{p} - \mathbf{p}_i(t_0)) \quad (6)$$

We ignore in our study any collective phenomena which might be important, and we also ignore the quantum correlations and the nonperturbative properties of the strong interaction. With these simplifications, each particle moves freely as time proceeds, but collides occasionally with another particle if it comes close enough, i.e., within the distance determined by total cross section $\sqrt{\sigma_T/\pi}$. In the collision, both particles abruptly change their momenta according to the differential cross section and/or produce new particles depending on the branching ratio of the various final states. The particles emerging from the collision are again moving freely until they make a collision with another particle.

The Monte-Carlo simulation in general cascade code has several shortcomings:

- (i) The deterministic interpretation of the total cross section as a geometric criterion that decides whether two particles are colliding with each other or not is not a faithful representation of the quantum mechanical scattering process. It would be

more appropriate to use a collision probability as a function of the impact parameter based on a quantum transition amplitude.

- (ii) Another important issue is the assumption on the collision space-time: The two particles collide each other at their shortest distance or maximal force point(s). This assumption makes a big difference between a general (parton) cascade code and an simplified analytic solution scheme [8, 9] or a relaxation time method [14, 15, 16]. The collision in a cascade code occurs only if there is substantial rapidity difference and/or transverse momentum difference since the shortest distance or maximal force point(s) between particles can be achieved in rather far future if two particles have same rapidity unless they have relatively high transverse momentum. On the other hand, most of collisions come from the small angle scattering between comoving partons in an analytic solution, namely collisions occurs among those in same rapidity. We believe this collision condition should be relaxed to allow those collisions between particles even if they are not in closest distance.

We hope to address these issues in future publications.

3.1. Initial Distribution

It is very difficult to obtain a realistic initial distribution (6) for the simulation, because of the complexity of nuclear parton distributions and the dynamics governing the decoherence of the nuclear wavefunctions. The following choice is mainly governed by considerations of simplicity and easy implementation in the cascade code. Note that we are considering only head-on collisions, although our code is fully three-dimensional.

As far as the transverse phase space distribution is concerned, reasonable choices can be derived from the semiclassical picture [7]. We assume that the number of produced partons is proportional to the number of primary collisions so that the transverse spatial distribution of the produced partons has the imprint of the transverse parton distribution of the colliding nuclei. This assumption can be expressed as the probability distribution for the initial transverse position $(x, y) = (r_{\perp} \cos \phi, r_{\perp} \sin \phi)$:

$$P(x, y) = B \left(1 - \frac{r_{\perp}^2}{R^2}\right) \quad (7)$$

where R is the radius of the nuclei and B is a normalization constant. Once the transverse distance from the collision axis is selected, we can choose the azimuthal angle with equal probability over $(0, 2\pi)$.

Krasnitz, Nara and Venugopalan (KNV) [17] found that the transverse momentum distribution from the study of small x-physics is given by the formula,

$$\frac{1}{\pi R^2} \frac{dN}{dy d^2 p_{\perp}} = \frac{1}{g^2} f_n(p_{\perp}/\Lambda_s) \quad (8)$$

where

$$\begin{aligned} f_n(p_{\perp}/\Lambda_s) &= \frac{a_1}{\exp(\sqrt{p_{\perp}^2 + m^2}/T_{eff}) - 1}, & p_{\perp} < 3\Lambda_s, \\ &= a_2 \Lambda_s^4 \ln(4\pi p_{\perp}/\Lambda_s) p_{\perp}^{-4}, & p_{\perp} > 3\Lambda_s \end{aligned} \quad (9)$$

where $a_1 = 0.0295$, $a_2 = 0.0343$, $m = 0.067\Lambda_s$, $T_{eff} = 0.93\Lambda_s$. y is rapidity and the saturation momentum $\Lambda_s = 1\text{GeV}$ in RHIC and 2GeV in LHC.

It is known that the rapidity of the produced particles after a heavy-ion collision is flat in the central rapidity region so that the rapidity y can be chosen from a constant distribution within the interval $y_{min} < y < y_{max}$. Once we have chosen the rapidity, the longitudinal momentum is given by the relation

$$p_z = \sqrt{m^2 + p_T^2} \sinh y. \quad (10)$$

We further assume that all of the primary collisions occur in the reaction plane, $z = 0$, at time $t = 0$ and the produced partons are born at the proper time, $\tau_0 = \sqrt{t^2 - z^2}$, where τ_0 is about $0.3 \text{ fm}/c$ at RHIC and $0.13 \text{ fm}/c$ at the LHC. We thus can find the initial time and longitudinal position of a produced parton once its rapidity is given, by calculating its velocity $\beta_z = p_z/E$ and setting $\beta_z = z/t$ to obtain t and z at the formation time τ_0 . For simplicity, we initialize all partons at a common time $t' = \tau_0$ and at $z' = \beta_z \tau_0$. However, we do not allow the partons interact, until they reach a proper time τ larger than the formation time τ_0 .

We assume that the number density per rapidity of produced partons is in the range $dN/dy \approx 1000 \sim 1500$.

3.2. Cross Sections

The dynamics enters into the Boltzmann equation through the total and differential cross section among partons. Differential cross sections at leading order α_s for the processes are stated here explicitly for convenience, although they have been given elsewhere [18],

$$\frac{d\sigma^{gg \rightarrow gg}}{dt} = \frac{9\pi\alpha_s^2}{2s^2} \left(3 - \frac{tu}{s^2} - \frac{su}{t^2} - \frac{st}{u^2} \right) \quad (11)$$

$$\frac{d\sigma^{gg \rightarrow q_a \bar{q}_b}}{dt} = \frac{\pi\alpha_s^2}{6s^2} \delta_{ab} \left(\frac{u}{t} + \frac{t}{u} - \frac{9}{4} \frac{t^2 + u^2}{s^2} \right) \quad (12)$$

$$\frac{d\sigma^{gq \rightarrow gq}}{dt} = \frac{4\pi\alpha_s^2}{9s^2} \left(-\frac{u}{s} - \frac{s}{u} + \frac{9}{4} \frac{s^2 + u^2}{t^2} \right) \quad (13)$$

$$\frac{d\sigma^{q_a q_b \rightarrow q_a q_b}}{dt} = \frac{4\pi\alpha_s^2}{9s^2} \left[\frac{s^2 + u^2}{t^2} + \delta_{ab} \left(\frac{t^2 + s^2}{u^2} - \frac{2}{3} \frac{s^2}{ut} \right) \right] \quad (14)$$

$$\frac{d\sigma^{q_a \bar{q}_b \rightarrow q_c \bar{q}_d}}{dt} = \frac{4\pi\alpha_s^2}{9s^2} \left[\delta_{ac} \delta_{bd} \frac{s^2 + u^2}{t^2} + \delta_{ab} \delta_{cd} \frac{t^2 + u^2}{s^2} - \delta_{abcd} \frac{2}{3} \frac{u^2}{st} \right] \quad (15)$$

$$\frac{d\sigma^{q_a \bar{q}_b \rightarrow gg}}{dt} = \frac{32\pi\alpha_s^2}{27s^2} \delta_{ab} \left[\frac{u}{t} + \frac{t}{u} - \frac{9}{4} \frac{t^2 + u^2}{s^2} \right] \quad (16)$$

and

$$\frac{d\sigma^{g\bar{q} \rightarrow g\bar{q}}}{dt} = \frac{d\sigma^{gq \rightarrow gq}}{dt}, \quad \frac{d\sigma^{\bar{q}\bar{q} \rightarrow \bar{q}\bar{q}}}{dt} = \frac{d\sigma^{qq \rightarrow qq}}{dt}. \quad (17)$$

We note that Eq.(11, 12, 14, 16) are symmetric under the exchange of $u \leftrightarrow t$ as dictated by the indistinguishability of the identical particles. The classical cross sections must therefore include an overall factor $1/2$.

To get total cross sections, we integrate analytically the differential cross sections using the conditions, $E_{cm} > 1$ GeV and the minimum momentum transfer $p_{\perp} > 0.5$ GeV so that the scattering angle θ in the CM frame should satisfy the condition $|\sin \theta| > (0.5 \text{ GeV})/E$, where E is the energy of the particle in CM frame. With this limitation on the scattering angle, we find $\sigma_{gg \rightarrow gg} \approx 10/\text{GeV}^2$ and $\sigma_{qq \rightarrow qq} \approx 0.6/\text{GeV}^2$ and $\sigma_{gq \rightarrow gq} \approx 0.7/\text{GeV}^2$ for the strong coupling constant $\alpha_s = 0.3$, which we will use throughout this work. These total cross sections are optimistic values for those perturbative processes because we choose low values for minimum CM energy as well as minimum momentum transfer. However, we note that about similar values for the cross section have been used by others [19, 6]

We use the following approximation for the $gg \rightarrow ggg$ cross section [10],

$$\begin{aligned} \frac{d\sigma^{gg \rightarrow ggg}}{dq_{\perp}^2 dy dk_{\perp}^2} &= \frac{9C_A \alpha_s^3}{2} \frac{q_{\perp}^2}{(q_{\perp}^2 + \mu_D^2)^2} \\ &\times \frac{\Theta(k_{\perp} \lambda_f - \cosh y) \Theta(\sqrt{s} - k_{\perp} \cosh y)}{k_{\perp}^2 \sqrt{(k_{\perp}^2 + q_{\perp}^2 + \mu_D^2)^2 - 4k_{\perp}^2 q_{\perp}^2}} \end{aligned} \quad (18)$$

where q_{\perp} is the momentum transfer of two colliding gluons and k_{\perp} the perpendicular momentum of the radiated gluon and y is its rapidity. $C_A = 3$ for the SU(3) gauge group, μ_D is a Debye screening mass, and λ_f is the mean free path. The first step function represents the Landau-Pomeranchuk-Migdal(LPM) effect while the second one is the energy constraint of the radiated gluon.

In order to integrate (18), we need several approximations, which we discuss now. For the Debye mass we use the value that is consistent with the $gg \rightarrow gg$ cross section:

$$\mu_D^2 = 2\pi C_{gg} \alpha_s^2 / \sigma_T^{gg \rightarrow gg}, \quad (19)$$

where $C_{gg} = 3$. This approximation gives us $\mu_D \approx 0.4$ GeV for $\sigma_{gg \rightarrow gg} = 10/\text{GeV}^2$. The mean free path, λ_f , is defined as $1/(\rho \sigma_T)$ where ρ is the density of particles and σ_T is the average total cross section of the parton. This is a dynamical variable even if we fix the total cross section, because the system is rapidly expanding. We can estimate the initial density for heavy ion collision to be $0.34 \sim 0.5/\text{GeV}$ with $4000 \sim 6000$ gluons at $\tau_0 = 0.3 \text{ fm}/c$ so that the mean free path is $0.2 \sim 0.3/\text{GeV}$. But this number quickly increases as the system expands. As a reasonable approximation we choose $\lambda_f = 1.0/\text{GeV}$ in our study. With these two parameter choices, we can integrate the differential cross section numerically. Using the Runge-Kutta algorithm, we evaluate the total cross section $\sigma_T^{gg \rightarrow ggg} \approx 3.6/\text{GeV}^2$

We can add the total cross section of each process to get the total cross section, e.g.,

$$\sigma_T^{gg} = \sigma_T^{gg \rightarrow gg} + \sigma_T^{gg \rightarrow ggg} + \sigma_T^{gg \rightarrow u\bar{u}} + \sigma_T^{gg \rightarrow d\bar{d}} + \sigma_T^{gg \rightarrow s\bar{s}}. \quad (20)$$

This total cross section will be used to decide whether two coming gluons will collide or not, by the criterion whether the impact parameter between two gluons in the reaction plane is less than $\sqrt{\sigma_T/\pi}$ or not. Once it is determined that a collision takes place, we can use the branching ratio to select which channel will become active. After we choose the channel, we can use the differential cross section of the channel to select a scattering angle and momentum transfer.

3.3. Basic Algorithm

We first select the global laboratory frame as the reference frame in which the simulation is performed. We next consider all possible pairs of particles and calculate their impact parameter b . The impact parameter is defined as the shortest distance between two particles in their reaction frame, i.e. their mutual CM frame with one particle moving in the $+z$ direction and the other moving in the $-z$ direction. To determine b , we apply an appropriate Lorentz transformation to each pair of particles. Suppose the particle 1, which has the position (x_1, y_1, z_1) , moves along the $+z$ -axis and particle 2, at (x_2, y_2, z_2) , moves along the $-z$ -axis in the reaction frame. The impact parameter is explicitly given by:

$$b = \sqrt{(x_1 - x_2)^2 + (y_1 - y_2)^2}. \quad (21)$$

We check whether a collision is possible by applying the criterion $b < \sqrt{\sigma_T/\pi}$ as discussed before. We also check whether the condition $z_1 < z_2$ is met.

For a given particle, there maybe are many possible collisions but we keep only the earliest one, as observed in the laboratory frame. We next calculate where and when two particles will collide. In order to determine the collision point(s) for two particles, we make use of the ‘‘maximal force’’ principle, which is explained in detail in Appendix A. In brief, we postulate that the two particles are interacting through a retarded long-range field. This assumption is consistent with our use of lowest-order perturbative cross sections. We determine the point on each particle’s trajectory where the retarded force becomes maximal. In general, these points correspond to different times in the laboratory frame, as an expression of the fact that the forces among particles propagate no faster than the speed of light.

If the time difference between the two times corresponding to a single collision is greater than the mean free path, there is no collision between them, because they will be interrupted by neighboring particles. This can reduce the number of collisions substantially as the particle density goes up, or the relative CM energy of a particle pairs increases. This mechanism is similar to the procedure A of ref. [11] (restriction of the signal velocity). Here, however, we do not impose an *ad-hoc* cut on allowable collisions; rather, the finite signal velocity is embodied in the determination of the interaction points for each particle (see Appendix A).

We then put all the collision events in time sequence and execute the collisions one by one in the global time frame. After each collision, the collision sequence must

be updated, because the particles emerging from collision have different phase space coordinates than before.

3.4. Bulk Properties

Since we have the full phase space information of all of particles composing our system, we can, in principle, calculate all the properties of the system. In particular, we can define the particle number current and the energy-momentum tensor as follows,

$$N^\mu(x) = \int \frac{d^3p}{E} p_\mu f(x, \mathbf{p}), \quad (22)$$

$$T^{\mu\nu}(x) = \int \frac{d^3p}{E} p^\mu p^\nu f(x, \mathbf{p}). \quad (23)$$

The classical entropy current is defined as:

$$S^\mu(x) = - \int \frac{d^3p}{E} p^\mu f(x, \mathbf{p}) \ln f(x, \mathbf{p}). \quad (24)$$

We also find it helpful to calculate the absolute momentum function weighted by the distribution

$$\tilde{P}_x(\mathbf{r}, t) = \int d^3p |p_x| f(x, \mathbf{p}), \quad (25)$$

$$\tilde{P}_z(\mathbf{r}, t) = \int d^3p |p_z| f(x, \mathbf{p}). \quad (26)$$

Local kinetic equilibrium requires $\tilde{P}_x = \tilde{P}_z$.

The entropy of the system of classical particles cannot be calculated from (24) since the phase space of the test particles is given by a sum of δ -functions,

$$f(\mathbf{x}, \mathbf{p}, t) = \sum_i \delta(\mathbf{x} - \mathbf{x}_i(t)) \delta(\mathbf{p} - \mathbf{p}_i(t)), \quad (27)$$

where $(\mathbf{x}_i, \mathbf{p}_i)$ is the position and momentum of the i -th particle. In order to define a smooth phase space density we smear this distribution in phase space such that the uncertainty relation is satisfied. We choose a spatial volume of extension Δx and a momentum space volume of extension Δp such that $\Delta x \Delta p_x > 1$. We use the representations of the Dirac δ -function as a Gaussian:

$$\delta(x - x_i) \approx \sqrt{\frac{a}{\pi}} e^{-a(x-x_i)^2} \quad (28)$$

and smooth the probability up to a few nearest momentum bins and normalize the distribution so that the integrated particle probability remains unity. This is known as the coarse graining procedure and the entropy of a system is dependent on the procedure. In our calculation, we assign the probability, Eq.(28), up to the third nearest spatial bin from the position of the particle. Using this method, we calculate the one-particle entropy to be 3.2 for an isolated particle.

4. Results and Discussions

We are considering a system of which the total number of particles (gluons) is 6000. The particles have a flat rapidity distribution between +2 and -2. The total cross

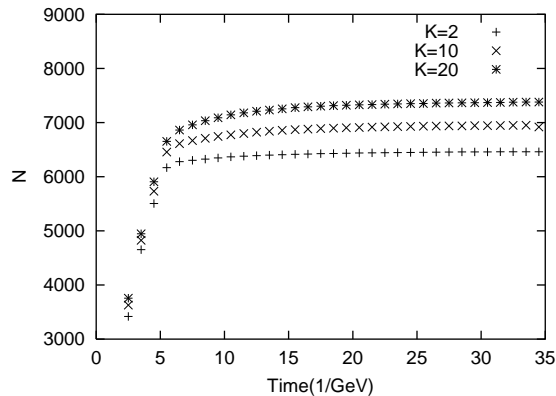


Figure 1. Total number of partons as a function of time in 1/GeV unit: 6000 initial gluons and $K = 2, 10, 20$. Data are average over 20 runs which use different random number sets.

section for the simulation has been calculated using the coupling constant $\alpha_s = 0.3$ and minimal momentum transfer 0.5 GeV as described before. We also include the effect of higher order diagrams in the form of a K-Factor $K = 2$. We use the KNV transverse momentum distribution (8,9) for the p_T distribution.

Figure 1 shows total number of particles as function of time. The primary partons are initialized at the proper time τ_0 ($= 1.5/\text{GeV}$ at RHIC energy), and the secondary partons are produced by collisions between primary partons of the system. In the following, when we use the term “produced partons”, we refer to those partons that are created in collisions within our transport code, but not to the initialized partons that are produced before the start of our transport calculation. With our parameters, the secondary partons, mostly gluons, are not produced as abundantly as predicted in the analytical estimate of Baier, Mueller, Schiff and Son [9]. One reason for this difference is that the cross section (18) is small at early times due to the influence of the LPM effect, which provides for a strong suppression of radiation at high density.

Figure 2 shows the ratio between transverse momentum and longitudinal momentum of the particles in a small box, which has the size of $2 \times 2 \times 1 \text{ fm}^3$ and is located at the coordinate origin, as a function of time. This ratio should be close to unity when the kinetic equilibration is reached. The figure shows that the ratio is increasing beyond unity, implying that the system is thinning more rapidly along the collision axis than in the transverse direction for $K = 2$ and even for $K = 10$. Kinetic equilibration can be achieved for the unrealistically large cross section with $K = 20$.

Figure 3 shows the energy density of the box as a function of time. The high energy particles escape from the box very quickly and a relatively slow expansion follows.

Figure 4 shows the particle number density of the box which we are considering as a function of time. We can see that more and more particles are staying in the box as the cross section gets larger, but the densities are almost the same after those high momentum particles escape. Scattering occurs only occasionally as time goes on.

In conclusion, we do not observe kinetic equilibration for a realistic cross section

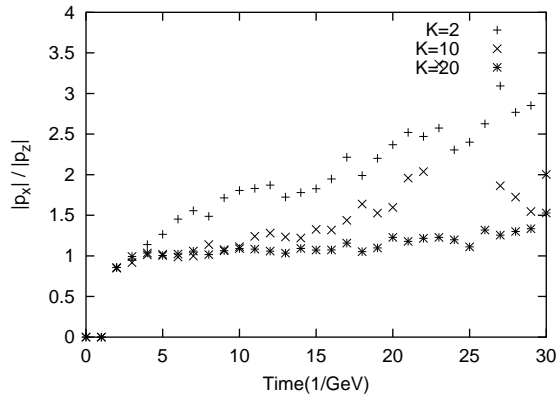


Figure 2. $\sum |p_x| / \sum |p_z|$ as a function of time in 1/GeV unit: 6000 initial gluons and K-Factor = 2(+), 10(x) and 20(*). Data are the average over 20 runs in which each run uses different set of random numbers. A small box ($2 \times 2 \times 1 fm^3$) at center is used for measurement.

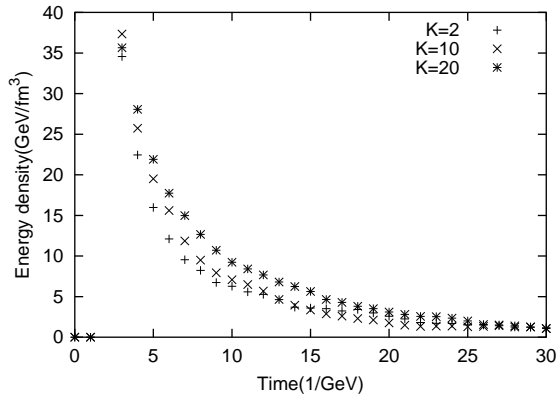


Figure 3. The energy density per fm^3 in the box at central region as a function of time .

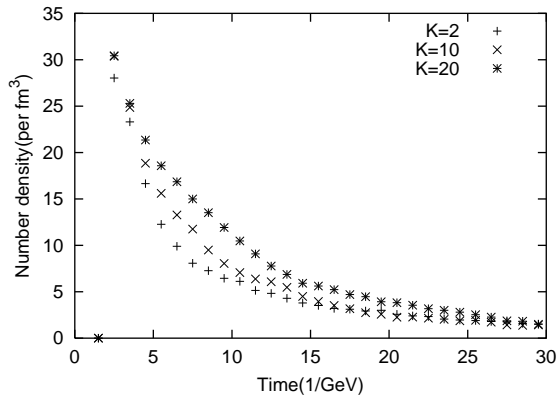


Figure 4. The number density per fm^3 in the box at central region as a function of time .

in our simulations. However, when we increase the cross section substantially (10 – 20 times!) approximate isotropy of the momentum distribution can be achieved. In our investigation here, we kept the low-momentum fixed. On the other hand, dynamical screening in an expanding medium provides an effective low-momentum cutoff that varies with time. This raises the question whether a selfconsistent treatment, in which the time-dependent density is used to determine the time variation of the total cross section, can exhibit an approach to equilibrium without unrealistic assumptions. We hope to return to this question, as well as to the issue of including $3 \rightarrow 2$ processes to ensure detailed balance, in a future publication.

Acknowledgments

G. R. Shin thanks the members of the Department of Physics at Duke University for their warm hospitality during his sabbatical visit. We both thank S. A. Bass, D. K. Srivastava, and S. Mrowczynski for helpful discussions and comments. This work has been supported in part by DOE grant DE-FG02-96ER40945 and by Andong National University.

Appendix A. Collision points

Quantum mechanics does not allow us to determine the precise moment of when a collision between two particles occurs due to the uncertainty relation. Here, we discuss this question in the context of classical mechanics, in particular, in classical electrodynamics. Consider two particles with charges q_1, q_2 , and positions and velocities, (x^μ, u^μ) and (r^ν, v^ν) , respectively. The electromagnetic field induced by particle 2 at the position of particle 1 is given by [20]

$$F^{\mu\nu}(x) = \frac{e}{[v \cdot (x - r(\tau'_x))]^3} [(x - r(\tau'_x))^\mu v^\nu - (x - r(\tau'_x))^\nu v^\mu] \quad (\text{A.1})$$

where $r(\tau'_x)$ is the source point associated with the field at point x . Each particle moves along its trajectory at constant velocity:

$$x^\mu = a^\mu + u^\mu \tau, \quad (\text{A.2})$$

$$r^\mu = b^\mu + v^\mu \tau'. \quad (\text{A.3})$$

Using the retardation condition, we can obtain the proper time of the source point for the field point x :

$$\tau'_x = (x - b) \cdot v - \sqrt{[(x - b) \cdot v]^2 - (x - b)^2}. \quad (\text{A.4})$$

The force on particle 1 due to the field of particle 2 is given by

$$F^{\mu\nu} u_\nu = \frac{e[(x - r')^\mu v \cdot u - (x - r') \cdot u v^\mu]}{[[(a - b + u\tau) \cdot v]^2 - (a - b + u\tau)^2]^{3/2}} \quad (\text{A.5})$$

where $r' = r(\tau'_x)$. This force will be maximal when the denominator is minimal. This condition will be met at

$$\tau_0 = \frac{(a-b) \cdot v(u \cdot v) - (a-b) \cdot u}{u^2 - (u \cdot v)^2}. \quad (\text{A.6})$$

Even though the classical collision occurs gradually, we associate this space-time point with the collision moment of the particle 1:

$$x^\mu = a^\mu + u^\mu \tau_0. \quad (\text{A.7})$$

Using the same procedure, we obtain the maximal force on particle 2 by the particle 1 at the proper time

$$\tau'_0 = \frac{(b-a) \cdot u(v \cdot u) - (b-a) \cdot v}{v^2 - (u \cdot v)^2} \quad (\text{A.8})$$

and the collision space-time point

$$r^\mu = b^\mu + v^\mu \tau'_0. \quad (\text{A.9})$$

Since the definitions of τ_0 and τ'_0 are manifestly Lorentz invariant, the interaction points are independent of the reference frame in which the two-body collision is calculated.

The force between the two particle is more complex due to the presence of color degrees of freedom. However, in lowest-order perturbation theory, the space-time behavior of the QCD force is identical to that in electrodynamics. We can thus apply the equations derived above.

Appendix B. Monte Carlo Sampling

We explain here the Monte-Carlo sampling for the process $gg \rightarrow gg$ only. The other processes are the same except the process $gg \rightarrow ggg$ which we discuss briefly at the end. We change the variable from the Mandelstam t to $\eta = \cos \theta$. The differential cross section becomes

$$\frac{d\sigma^{gg \rightarrow gg}}{d\eta} = \frac{9\pi\alpha_s^2}{4E_{cm}^2} \left[3 - \frac{(1-\eta)(1+\eta)}{4} + 2\frac{1+\eta}{(1-\eta)^2} + 2\frac{1-\eta}{(1+\eta)^2} \right] \quad (\text{B.1})$$

where η is confined by the minimal momentum transfer Q_0 which we will choose either 0.5 or 1GeV. The total cross section can be obtained analytically by integrating over the allowed range. The natural way to choose η by monte Carlo method is that we calculate

$$r = \int_{\eta_{min}}^{\eta} \frac{d\sigma}{d\eta} \quad (\text{B.2})$$

and invert this equation to solve for η . Since this is not easy to do, we divide the (η_{min}, η_{max}) into several intervals. Each interval can be integrated over analytically to give an area. We generate a random number r_1 and select the interval depending on the area, i.e., if $r_1 < s_1/\sigma_T$, the interval 1 is chosen, and so forth. Once we have selected

the interval $(\eta_{start}, \eta_{end})$, we can find the straight line connecting the points at η_{start} and η_{end} and choose η between $(\eta_{start}, \eta_{end})$ by linear random sampling and then use the accept-reject method. This triple Monte Carlo sampling gives a satisfactory result.

The sampling of the $gg \rightarrow ggg$ process is slightly more complicated. Using the step function in (18), we find the rapidity of the bremsstrahlung gluon, (y_{min}, y_{max}) , where for a given CM energy \sqrt{s} ,

$$y_{max} = \ln \left(\sqrt{\sqrt{s}\lambda_f} + \sqrt{\sqrt{s}\lambda_f - 1} \right). \quad (\text{B.3})$$

Once we have chosen the rapidity, we have

$$\left(\frac{\cosh y}{\lambda_f} \right)^2 < k_{\perp}^2 < \left(\frac{\sqrt{s}}{\cosh y} \right)^2 \quad (\text{B.4})$$

and

$$0 < q_{\perp}^2 < s. \quad (\text{B.5})$$

Again, we can use the accept-reject method to sample $(k_{\perp}^2, q_{\perp}^2)$. This algorithm generates an acceptable distribution within a reasonable CPU time.

References

- [1] Bjorken J D 1983 *Phys. Rev. D* **27** 140
- [2] Baym G 1984 *Phys. Lett.* **138B** 18
- [3] Geiger K and Müller 1992 B *Nucl. Phys.* **B369** 600; Geiger K 1992 *Phys. Rev. D* **46** 4965, 4986; Geiger K and Kapusta J I 1993 *Phys. Rev. D* **47** 4905
- [4] Geiger K 1995 *Phys. Rept.* **258** 237
- [5] Zhang B 1997 *Comp. Phys. Comm.* **109** 70; Zhang B and Pang Y 1997 *Phys. Rev. C* **56** 2185; Zhang B, Gyulassy M and Pang Y 1998 *Phys. Rev. C* **58** 1175
- [6] Molnar D and Gyulassy M 2000 *Phys. Rev. C* **62** 054907
- [7] McLerran L and Venugopalan R 1994 *Phys. Rev. D* **49** 2233, 3352, **50** 2225
- [8] Bjorker J and Venugopalan R 2001 *Phys. Rev. C* **63** 024609; *Preprint* hep-ph/0011001
- [9] Baier R, Mueller A H, Schiff D, and Son D T 2001 *Phys. Lett. B* **502** 51
- [10] Biro T S, van Doorn E, Müller B, Thoma M H, and Wang X N 1993 *Phys. Rev. C* **48** 1275
- [11] Kortemeyer G, Bauer W, Haglin K, Mullay J, and Pratt S 1995 *Phys. Rev. C* **52** 2714
- [12] de Groot S R, van Leeuwen W A, and van Weert C G 1980 *Relativistic Kinetic Theory* (Amsterdam: North-Holland)
- [13] Csernai L P 1994 *Introduction to Relativistic Heavy Ion Collisions* (New York: John Wiley & Sons)
- [14] Mueller A H 2000 *Nucl. Phys.* **B572** 227
- [15] Nayak G C, Dumitru A, McLerran L, and Greiner W 2001 *Nucl. Phys.* **A687** 457
- [16] Serreau J and Schiff D 2001 *J. High Energy Phys.* JHEP11(2001)039
- [17] Krasnitz A and Venugopalan R 2000 *Phys. Rev. Lett.* **84** 4309; Krasnitz A and Venugopalan R 2001 *Phys. Rev. Lett.* **86** 1717; Krasnitz A, Nara Y, and Venugopalan R *Phys. Rev. Lett.* **87** 192302
- [18] Itzykson C and Zuber J B 1980 *Quantum Field Theory* (New York: McGraw Hill)
- [19] Nara Y, Vance S E and Csizmadia P 2002 *Phys. Lett. B* **531** 209
- [20] Jackson J D 1998 *Classical Electrodynamics* (New York: John Wiley & Sons)